




OPEN

Functional network topology of the right insula affects emotion dysregulation in hyperactive-impulsive attention-deficit/hyperactivity disorder

Tammo Viering^{1,2}, Pieter J. Hoekstra², Alexandra Philipsen³, Jilly Naaijen^{4,5}, Andrea Dietrich², Catharina A. Hartman⁶, Jan K. Buitelaar^{4,5,7}, Andrea Hildebrandt⁸, Carsten Gießing^{1,11} & Christiane M. Thiel^{1,9,10,11}

Emotion dysregulation is common in attention-deficit/hyperactivity disorder (ADHD). It is highly prevalent in young adult ADHD and related to reduced well-being and social impairments. Neuroimaging studies reported neural activity changes in ADHD in brain regions associated with emotion processing and regulation. It is however unknown whether deficits in emotion regulation relate to changes in functional brain network topology in these regions. We used a combination of graph analysis and structural equation modelling (SEM) to analyze resting-state functional connectivity in 147 well-characterized young adults with ADHD and age-matched healthy controls from the NeuroIMAGE database. Emotion dysregulation was gauged with four scales obtained from questionnaires and operationalized through a latent variable derived from SEM. Graph analysis was applied to resting-state data and network topology measures were entered into SEM models to identify brain regions whose local network integration and connectedness differed between subjects and was associated with emotion dysregulation. The latent variable of emotion dysregulation was characterized by scales gauging emotional distress, emotional symptoms, conduct symptoms, and emotional lability. In individuals with ADHD characterized by prominent hyperactivity-impulsivity, the latent emotion dysregulation variable was related to an increased clustering and local efficiency of the right insula. Thus, in the presence of hyperactivity-impulsivity, clustered network formation of the right insula may underpin emotion dysregulation in young adult ADHD.

¹Biological Psychology, Department of Psychology, School of Medicine and Health Sciences, Carl-von-Ossietzky Universität Oldenburg, Postfach 2503, 26111 Oldenburg, Germany. ²Department of Child and Adolescent Psychiatry, University Medical Center Groningen, University of Groningen, Groningen, The Netherlands. ³Department of Psychiatry and Psychotherapy, University of Bonn, Bonn, Germany. ⁴Department of Cognitive Neuroscience, Donders Institute for Brain, Cognition and Behaviour, Radboud University Medical Center, Nijmegen, The Netherlands. ⁵Centre for Cognitive Neuroimaging, Donders Institute for Brain, Cognition and Behaviour, Radboud University, Nijmegen, The Netherlands. ⁶Department of Psychiatry, Interdisciplinary Center Psychopathology and Emotion Regulation, University Medical Center Groningen, University of Groningen, Groningen, The Netherlands. ⁷Karakter Child and Adolescent Psychiatry University Centre, Nijmegen, The Netherlands. ⁸Psychological Methods and Statistics, Department of Psychology, School of Medicine and Health Sciences, Carl-von-Ossietzky Universität Oldenburg, Oldenburg, Germany. ⁹Research Center Neurosensory Science, Carl-von-Ossietzky Universität Oldenburg, Oldenburg, Germany. ¹⁰Cluster of Excellence "Hearing4all", Carl von Ossietzky Universität Oldenburg, Oldenburg, Germany. ¹¹These authors jointly supervised this work: Carsten Gießing and Christiane M. Thiel. ✉email: tammo.viering@uni-oldenburg.de

Attention-deficit/hyperactivity disorder (ADHD) is a neurodevelopmental disorder characterized by core symptoms of inattention and/or hyperactivity-impulsivity that may persist well into adulthood¹. Emotion dysregulation, although not a core symptom, is a frequently co-occurring clinical problem². Emotion dysregulation refers to the inability to adequately modulate and control emotions³. Its prevalence within the ADHD population changes with age, from 25 to 45% in children to 30–70% in adults, and its co-occurrence is associated with reduced well-being, risky behavior, and social impairments². Especially individuals with ADHD and impulsivity-hyperactivity symptoms often suffer from emotion dysregulation⁴. However, the neural roots of ADHD associated emotion dysregulation remain unclear.

In emotion dysregulation, a distinction between explicit and implicit emotion regulation has been made. Explicit emotion regulation requires conscious effort and is commonly achieved by applying cognitive control and reappraisal strategies. While cognitive control and reappraisal are particularly associated with activity in structures of the ventral attention and frontoparietal network⁵, it is precisely these structures in which deviant—often reduced—activity is frequently found in childhood and adult ADHD studies¹. Implicit emotion regulation, on the other hand, is an unconscious stimulus-driven process based on experience-based reward estimations. The ventromedial prefrontal cortex and the anterior cingulate cortex have been linked to implicit emotion regulation⁵. With regard to ADHD, it appears that not only structures related to explicit emotion regulation, i.e. structures for cognitive control and reappraisal, are affected, but also those associated with implicit emotion regulation and rather fundamental emotion reactivity processes⁶. Functional connectivity studies consistently showed deviations in structures of the limbic system including the orbitofrontal, ventromedial prefrontal and anterior cingulate cortex in patients with ADHD^{7–13}. Also, task-based fMRI studies using emotion perception and processing tasks in individuals with ADHD found evidence for functional abnormalities in the amygdala and insula, possibly indicating increased bottom-up emotional reactivity^{14,15}. Task-based fMRI studies related to implicit emotion regulation, i.e., using fear extinction via habituation or emotional Stroop paradigms, which controlled for differences in cognitive control, found ADHD-specific differences in the ventral anterior cingulate and ventromedial prefrontal cortex^{16–18}. Given the heterogeneity of ADHD, existing neuroimaging studies, and postulated neurocognitive models, e.g., the dual-pathway model¹⁹, one might expect ADHD-associated emotion dysregulation to be similarly complex, with both explicit and implicit regulatory processes accounting for it.

While several studies, using task-based as well as resting state fMRI, reported brain activity deviations in structures commonly associated with emotion processing and emotion regulation, few have attempted to directly correlate corresponding activation patterns with emotion dysregulation and none has investigated changes specific to ADHD presentations. Two childhood ADHD studies used seed-based connectivity approaches focusing on the amygdala. They reported associations between high emotion dysregulation scores and reduced negative connectivity with the insula and frontoparietal structures as well as increased positive connectivity with the anterior cingulate cortex^{20,21}. Connectivity changes beyond the amygdala have, however, not been investigated, and it remains uncertain whether the reported associations are indeed ADHD- or possibly even ADHD presentation-specific.

To investigate the relationship between emotional dysregulation and functional brain network organization, we used graph theory to analyze fMRI resting-state data from healthy individuals and individuals with ADHD with and without hyperactivity-impulsivity symptoms. We captured the centrality of each brain network node and analyzed whether nodes were highly integrated and connected, either locally towards their direct neighboring nodes or globally with the entire network. Graph theory-based methods have previously been used in ADHD research^{10,11,13} to describe changes in network topology of functional connectivity. These studies show increased local connectivity and efficiency and decreased global integration. It is however unclear how such changes in information processing properties of brain networks relate to emotional deficits. We gauged emotional dysregulation through structural equation modelling (SEM), using a combination of several self and informant scales assessing emotional problems, emotional lability, and conduct problems as well as one experimental task of emotion recognition. SEM is particularly well suited for testing the significance of certain assumed (group-specific) relations while simultaneously estimating latent variables embedded within the relational model. We focused our analysis on nodal topology measures and aimed to identify those brain regions whose local, functional brain network integration specifically contributes to emotion dysregulation in predominantly inattentive ADHD (ADHD-I) and ADHD with symptoms of hyperactivity-impulsivity (ADHD-C/H).

We hypothesized that an ADHD-specific association exists between the functional brain network measures for local network integration and emotion regulation. Thereby, we focused on measures of network topology within frontoparietal and limbic brain regions that have previously been associated with emotion regulation and processing. We assumed that the strongest relation would be found in individuals with predominantly hyperactive-impulsive ADHD.

Results

Sample characteristics. Age and sex did not significantly differ between the ADHD and control group. Participants with ADHD showed higher scores on all four measures of emotional problems and dysregulation. Further, compared to controls, participants with ADHD had a significantly lower IQ, partially showed oppositional defiant disorder (ODD) or conduct disorder (CD) comorbid diagnoses and, in general, more often used stimulant medication. ADHD presentations groups did not significantly differ with regard to age, sex, IQ, the four measures of emotion dysregulation, or stimulant use. The demographic details of the sample are given in Table 1.

Group	ADHD				Controls versus ADHD group comparisons		
	Controls	Total	ADHD-I	ADHD-C/H			
	N = 91 M ± SD	N = 56 M ± SD	N = 31 M ± SD	N = 25 M ± SD	Test statistic	p-value	Effect-size
Age (years)	20.2 ± 3.5	19.6 ± 3.5	19.5 ± 3.8	19.7 ± 3.2	T = 1.004	0.317	d = 0.170
IQ (WISC/WAIS)	111.4 ± 13.2	95.9 ± 18.0	98.0 ± 17.7	93.2 ± 18.4	U = 3846	< 0.001	d = 0.501
ADHD, inattention symptoms ^a	0.5 ± 1.1	7.2 ± 1.4	7.2 ± 1.3	7.1 ± 1.6	U = 25.5	< 0.001	d = 0.990
ADHD, hyperactive-impulsive symptoms ^a	0.5 ± 0.9	5.0 ± 2.4	3.4 ± 1.9	7.0 ± 0.96	U = 291.5	< 0.001	d = 0.890
K-10 psychological distress	12.9 ± 3.6	19.7 ± 5.7	19.3 ± 5.8	20.3 ± 5.6	U = 795	< 0.001	d = 0.688
CPRS-R:L emotional lability	44.2 ± 3.3	50.9 ± 9.4	49.5 ± 8.4	52.6 ± 10.5	U = 1412	< 0.001	d = 0.446
SDQ emotional symptoms	1.7 ± 1.6	2.9 ± 2.5	3 ± 2.6	2.8 ± 2.3	U = 1897	0.008	d = 0.255
SDQ conduct symptoms	1.1 ± 1.1	2.1 ± 1.6	2.0 ± 1.6	2.2 ± 1.6	U = 1598	< 0.001	d = 0.373
	n	n	n	N			
Sex (male)	48 (53%)	36 (64%)	20 (65%)	16 (64%)	$\chi^2 = 1.443$	0.230	$\varphi_c = 0.010$
Stimulant user (yes)	3 (3%)	30 (54%)	22 (65%)	10 (40%)	$\chi^2 = 47.484$	< 0.001	$\varphi_c = 0.323$
DSM-IV ODD (K-SADS)	0 (0%)	13 (23%)	4 (13%)	9 (36%)	$\chi^2 = 20.384$	< 0.001	$\varphi_c = 0.139$
DSM-IV CD (K-SADS)	0 (0%)	3 (5%)	1 (3%)	2 (8%)	$\chi^2 = 2.658$	0.103	$\varphi_c = 0.018$

Table 1. Sample characteristics of the control and ADHD groups as well as of presentation-specific ADHD subgroups. Means between groups were compared with independent sample t-tests or Mann-Whitney-U-tests. Frequency distributions were compared with Pearson's Chi-square (χ^2)-test. For the CPRS-R:L t-scores are presented, while for the SDQ and K-10 the questionnaire scores are given. ADHD = Attention Deficit/Hyperactivity Disorder; ADHD-C/H: attention-deficit/hyperactivity disorder, combined or predominantly impulsive/hyperactive attention-deficit/hyperactivity disorder; ADHD-I: predominantly inattentive attention-deficit/hyperactivity disorder; CD = Conduct Disorder; CPRS-R:L = Conners' parent rating scale, revised, long version; DSM-IV = Diagnostic and Statistical Manual of Mental Disorders, 4th Edition; HC = Healthy Controls; IQ = Intelligence Quotient; K-SADS = Kiddie Schedule for Affective Disorders and Schizophrenia; K-10 = Kessler Psychological distress scale, NESDA version; N = number of participants; n = number of participants within subgroups; ODD = Oppositional Defiant Disorder; SD = Standard Deviation; SDQ = Strength and Difficulties Questionnaire; WAIS: Wechsler Adult Intelligence Scale; WISC: Wechsler Intelligence Scale for Children. ^aCombined symptom counts were derived from DSM-IV subscales of K-SADS and the Conners' rating scales.

Structural equation models. To identify brain regions in which emotion dysregulation is specifically linked with functional brain network topology as a function of ADHD presentation we combined graph analysis with SEM.

Variable selection. In a first step, several tasks, questionnaires, or questionnaire subscales that capture different aspects of emotion dysregulation were examined to identify variables for estimating a latent emotion dysregulation variable. To construct the latent emotion dysregulation variable, we used multi-group confirmatory factor analysis. Significant loadings for the constructed latent variable were found for the emotional distress scores of K-10 ($z = 6.008$, $p < 0.001$, $\beta = 0.909$), SDQ's emotional symptoms subscale ($z = 4.745$, $p < 0.001$, $\beta = 0.603$), SDQ's conduct symptoms subscale ($z = 3.734$, $p < 0.001$, $\beta = 0.546$), and CPRS-R:L's emotional lability subscale ($z = 3.044$, $p = 0.002$, $\beta = 0.428$). These variables were considered for the subsequent SEM, while MINDS-GERT for emotion recognition ($z = 0.019$, $p = 0.983$, $\beta = 0.002$) and ICU for callousness-unemotional traits ($z = 1.953$, $p = 0.051$, $\beta = 0.163$) were discarded. Compared to healthy controls ($s_{HC}^2 = 0.300$) and participants with ADHD-C/H ($s_{ADHD-C/H}^2 = 0.340$), latent variable variance of participants with ADHD-I (standardized variance, $s_{ADHD-I}^2 = 1$) was greatest.

Three-group structural equation model. Second, to identify group dependent differences between network topology and the latent variable gauging emotion dysregulation, we used three-group SEM and estimated regression parameters for the group-specific relationship between the latent emotion dysregulation variable and measures of nodal network topology. Pooling over different density levels of connectivity, the SEM revealed group differences in the relation between clustering coefficient as well as local efficiency measures, respectively, and the latent variable for emotion dysregulation in the right insula (see Fig. 1a). For participants with ADHD-C/H the regression parameter estimates of the SEM were greatest, while they were smallest for participants with ADHD-I (see Fig. 1b). Table 2 displays the group-specific z-values for the relation between the latent variable and the right insula's clustering and local efficiency measures. It also shows p-values (uncorrected), and parameter estimates of the completely standardized solution. Further, Table 2 gives model-specific χ^2 , degrees of freedom, p-values of the models, goodness-of-fit measures (CFI, SRMR, and RMSEA), p-values that are the result of the χ^2 difference tests between the main models and the corresponding models with fixed regression parameters, and significant pairs of the post-hoc two-group SEM.

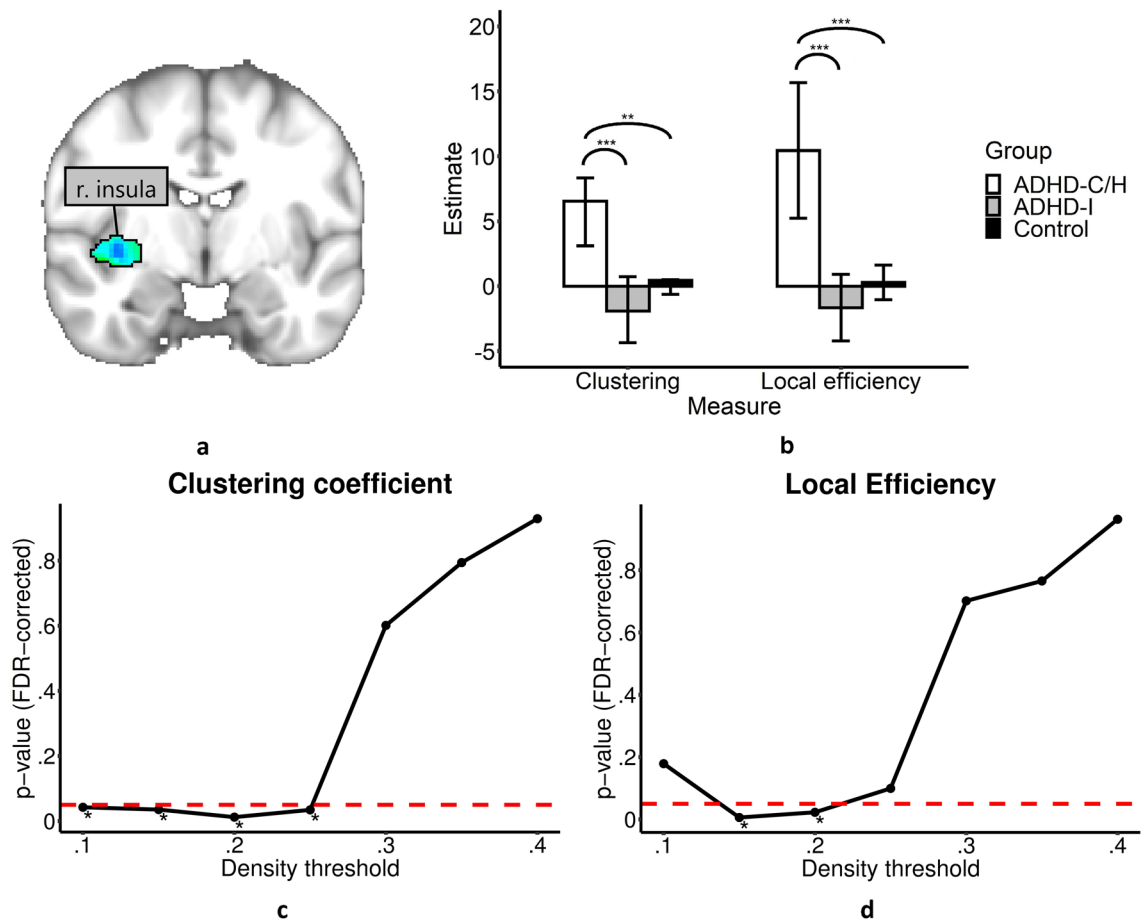


Figure 1. Brain nodes whose nodal network properties are associated with emotional dysregulation in young adult participants with ADHD. Results are shown for the latent variable in relation to local efficiency and clustering measures of the right insula. **(a)** The right insula showed a significant association with emotional dysregulation. Here the underlying parcel is shown. **(b)** Group-specific parameter estimates for the relation between the emotional latent variable and the topology measures (density-integrated) significantly differed between the participants with ADHD-I and ADHD-C/H as well as between participants with ADHD-C/H and controls. 95% confidence interval are displayed. Asterisks give significant group-specific differences (as calculated with χ^2 difference tests) of the corresponding post-hoc two-group SEM ($***p < 0.001$, $**p < 0.01$, $*p < 0.05$, n.s. $p > 0.05$; ADHD-C/H: attention-deficit/hyperactivity disorder, combined or predominantly impulsive/hyperactive attention-deficit/hyperactivity disorder; ADHD-I: predominately inattentive attention-deficit/hyperactivity disorder). **(c, d)** Group-specific differences in the relation between the latent variable and topology measures exist across graphs with different density thresholds (below 0.25). p -values of the χ^2 difference tests are shown. Asterisks signify significance after FDR-correction. The dashed red line represents $p = 0.05$. Figure **(a)** was created using FSLeys (version 0.22.6, <https://fsl.fmrib.ox.ac.uk/fsl/fslwiki/FSLeys>). Figures **(b, c, and d)** were created with R software (version 3.6.0, <https://cran.r-project.org/>).

Only in the ADHD-C/H group were the topology measures of the insula significantly related to emotion dysregulation. The respective models showed satisfactory goodness-of-fit measures. Results were highly significant for the density-integrated models and significant group-specific differences were found across multiple density thresholds below 25% connectivity (see Fig. 1c, d). Results for SEM with clustering coefficients and local efficiency were very similar, as the measures themselves are very similar. Correspondingly, both measures, at the integrated level, showed a correlation of 0.913 for the right insula. Post-hoc two-group comparisons revealed significant group differences between the participants with ADHD-I and ADHD-C/H as well as between participants with ADHD-C/H and controls. For the other nodal topology measures no significant results were found in the right insula.

While not surviving FDR-controlling procedures on the integrated level, SEM with density thresholds between 35 and 40% connectivity revealed group differences in the relationship between eigenvector centrality and the latent variable for emotion dysregulation in the right DLPFC. For participants with ADHD-C/H the regression parameter estimates of the SEM were greatest, while they were smallest for healthy controls. Significant group-specific differences in the relation between topology measures and emotion dysregulation on the uncorrected level occurred for measures of nodes in the right ventromedial prefrontal cortex, frontal pole, right insula, right anterior mid-cingulate cortex, and left insula (all uncorrected p -values < 0.01). For none of the other regions

Measure	Density	HC			ADHD-I			ADHD-C/H			χ^2	df	p-value	Fit-measures CFI SRMR RMSEA	χ^2 difference test p-value (FDR- corr.)	Sig. pairs in Post-hoc χ^2 difference tests (Bonferroni- corr.)
		z	p-value	β	z	p-value	β	z	p-value	β						
Right insula																
Cluster- ing	0.10	-0.609	0.543	-0.060	-0.167	0.868	0.543	3.512	<0.001	0.754	25.652	21	0.220	0.944 0.880 0.067	0.042	HC vs. ADHD-C/H ADHD-I vs. ADHD-C/H
	0.15	-0.483	0.629	-0.246	-1.453	0.146	-0.246	3.308	0.001	0.735	26.140	21	0.201	0.939 0.087 0.071	0.035	HC vs. ADHD-C/H ADHD-I vs. ADHD-C/H
	0.20	1.539	0.124	0.172	-2.110	0.035	-0.366	3.293	0.001	0.734	23.578	21	0.314	0.970 0.075 0.050	0.012	HC vs. ADHD-I HC vs. ADHD-C/H ADHD-I vs. ADHD-C/H
	0.25	1.256	0.209	0.140	-2.206	0.027	-0.392	3.339	0.001	0.733	21.857	21	0.408	0.990 0.063 0.029	0.034	HC vs. ADHD-I HC vs. ADHD-C/H ADHD-I vs. ADHD-C/H
	Inte- grated	0.820	0.412	0.091	-1.559	0.119	-0.279	3.746	<0.001	0.844	23.472	21	0.319	0.971 0.075 0.049	0.008	HC vs. ADHD-C/H ADHD-I vs. ADHD-C/H
Local efficiency	0.15	-1.086	0.277	-0.108	-1.322	0.186	-0.215	3.730	<0.001	0.830	25.535	21	0.225	0.948 0.084 0.066	0.005	HC vs. ADHD-C/H ADHD-I vs. ADHD-C/H
	0.20	1.435	0.151	0.158	-1.761	0.078	-0.301	3.297	0.001	0.740	22.604	21	0.365	0.980 0.073 0.039	0.023	HC vs. ADHD-C/H ADHD-I vs. ADHD-C/H
	Inte- grated	0.424	0.672	0.046	-1.259	0.208	-0.222	3.919	<0.001	0.882	23.693	21	0.308	0.969 0.078 0.051	0.005	HC vs. ADHD-C/H ADHD-I vs. ADHD-C/H

Table 2. Results of multi-group structural equation model analysis. Significant results after FDR-correction are given for the SEM with local efficiency, clustering coefficient of the right insula. All but the last column refer to the three-group SEM with group-specific regression parameter estimates. Group-specific z-statistics for the relation between the latent emotion dysregulation variable and the topology measures, parameter-specific p-values (uncorrected), which were obtained by using the quotient of the estimates and their standard error as a test statistic, and β estimates of the completely standardized solution are displayed for significant density-integrated models and the corresponding density-specific models (as calculated with χ^2 -difference tests). The table also displays model-specific χ^2 , degrees of freedom, p-values of the models, goodness-of-fit measures (CFI, SRMR, and RMSEA), p-values that are the result of χ^2 difference tests between the main models and the corresponding models with fixed regression parameters, and significant pairs of the post-hoc two-group SEM. Significant two-group differences mainly exist between the ADHD-C/H group and the other two groups. ADHD-C/H: combined or predominantly impulsive/hyperactive attention-deficit/hyperactivity disorder; ADHD-I: predominately inattentive attention-deficit/hyperactivity disorder; HC: healthy controls.

examined did we find significant group-specific differences in the relationship between the latent emotion dysregulation variable and measures of nodal network topology.

Additional analyses. Robustness of the results was controlled by evaluating the group-specific differences in overall connectivity strength of the individual networks. The analysis of overall connectivity did not reveal significant group differences. Finally, the multi-group SEM analysis was repeated using an alternative parcellation scheme to investigate the robustness of the results with respect to the chosen parcellation. The repetition of the main analysis with an alternative parcellation scheme revealed a group-specific difference in the relation between the clustering or local efficiency, respectively, and emotion dysregulation in the right insula. Further significant differences were found for the left insula and the right ventromedial prefrontal cortex and frontal pole. The significant frontal pole difference also showed for the density-integrated values and after applying FDR-controlling procedures (clustering coefficient: $p = 0.047$, FDR-corrected; see Supplementary Table S1). The significant right insula result, however, was not revealed using threshold-integrated values but only with a density threshold of 25% connectivity and not after FDR-controlling procedures (clustering coefficient: $p = 0.033$, uncorrected; local efficiency: $p = 0.030$, uncorrected).

Discussion

Emotion dysregulation is a key component of many psychiatric conditions, including young adult ADHD. We identified properties of functional brain network topology related to a latent measure of emotion dysregulation by using a combination of graph theoretical methods with structural equation modelling. Our results provide evidence that only in individuals with ADHD-C/H emotion dysregulation is accompanied by increases in local efficiency and clustering of the right insula.

Local efficiency and clustering measure how interconnected a node's neighbors are to each other. Increases imply stronger functional connections between structures directly connected to the respective brain region. Here the insula was identified as showing increased connections to its nearest neighbors contributing to emotion dysregulation in ADHD-C/H. The insula integrates interoceptive states with emotional information via connections to other limbic regions such as the amygdala²². It plays an essential role in implicit emotion regulation via reciprocal connections with the ventromedial prefrontal cortex and other regions particularly associated with experience-based reward estimations²³. Throughout brain maturation, functional network formation is characterized by specific patterns of integrative and segregating processes²⁴. These processes are also reflected in measures such as the clustering coefficient and local efficiency. Local efficiency in particular has previously been used as a measure of local brain segregation and it was suggested that increased local efficiency goes along with a loss of global brain network integration. For example, it was shown that higher local efficiency is associated with lower global efficiency and reduced performance during cognitive tasks²⁵. Prior research consistently provides evidence of delays in the neural maturation of individuals with ADHD^{7,26,27}. Increases in the insula's clustering and local efficiency, i.e. functional connectivity increases between neighboring nodes, may indeed, originate from reduced or delayed network-forming processes. This may negatively affect the efficiency with which the insula performs its integrative tasks and helps to appropriately evaluate emotional stimuli or to facilitate emotion regulation. Our results may reflect ADHD presentation-specific deficiencies in functional network forming processes. At the behavioral level, this could lead to inappropriate behavior and some of the commonly observed emotional problems in ADHD.

The positive association between the functional connectivity of structures directly connected to the insula, i.e. local efficiency and clustering, and emotional functioning in ADHD-C/H was neither found in healthy controls nor participants with ADHD-I. Our results are consistent with expectations, given that this subgroup was shown to be most severely affected by co-occurring emotion dysregulation⁴. Indeed, in the comparison of the different ADHD presentations, the combined type had shown local functional hyperconnectivity in regions associated with emotion processing and implicit emotion regulation, namely the vmPFC²⁸. Previously, it was observed that deviations of functional connectivity in ADHD-I occur most clearly in areas of the frontoparietal network, especially the dorsolateral prefrontal cortex, whereas for ADHD-C deviations are most pronounced in areas of the default mode network, i.e. in areas associated with motivation and emotion processing. Since ADHD-I is predominantly characterized by inattention symptoms, it has been suggested that problems in top-down control systems are more likely to underlie this presentation, whereas predominately combined ADHD appears to be more clearly associated with motivation and emotion processing networks²⁹. This could not be confirmed with the analysis carried out here. We found no evidence that nodal topology in top-down control regions would be associated with emotion dysregulation in ADHD-I. On the contrary, the right dorsolateral prefrontal cortex showed an ADHD-C/H dependent association between eigenvector centrality and emotion dysregulation. However, these results should be regarded with caution, as they were only seen at two density thresholds. Taken together, the clinical distinction between ADHD presentations with and without hyperactivity-impulsivity symptoms and the associated prevalence differences commonly observed in co-occurring problems such as emotion dysregulation may be reflected in differential deviations of the underlying functional organization of the brain.

Significant results were found for the *right* insula only. While ADHD is not understood as a generally right-lateralized disorder, some functions are more strongly associated with right hemisphere processing³⁰. Indeed, the right hemisphere is assumed to take a dominant role in emotion processing. Regarding the regulation of emotions, findings are not as conclusive. However, evidence concerning the insula suggests that processes for integrating interoceptive and emotional/motivational information are rather right lateralized³¹. Note that the left insula yielded—like the dorsolateral prefrontal cortex, right ventromedial prefrontal cortex, frontal pole and cingulate cortex—similar but weaker results, which did, however, not survive correction for multiple comparisons on the integrated level.

The latent variable for emotion dysregulation encompassed self-reported emotional distress, emotional and conduct symptoms and informant-reported emotional lability. Callous-unemotional traits and emotion recognition did not contribute significantly. Their relation to the other emotional measures (i.e., emotional distress and lability) appeared to be rather negligible. This is not surprising as callous-unemotional traits are characterized by deficient affect and lack of empathy, which is a conceptually different aspect of emotion³². While emotion recognition is an important prerequisite for the regulation of emotions, adolescents with and without emotion dysregulation have shown similar abilities in recognizing emotions, suggesting again a conceptual difference³³. Nevertheless, deficits in both are frequent in ADHD, a common occurrence is, however, not imperative³⁴.

The novel combination of SEM and graph theory presented here enabled us to reliably assess the functional network topology underlying emotion dysregulation. By using a SEM approach, it was possible to simultaneously determine emotional dysregulation as a latent variable of several emotion questionnaires and assess the group-specific relationships of emotion dysregulation with different measures of nodal brain topology. Previous approaches were limited in focusing on seed based functional connectivity of the amygdala only^{20,21} and using only unidimensional emotional measures. Compared to prior neuroimaging studies, we used a relatively large and well characterized sample of young adult ADHD participants and healthy controls. Also, cases with missing values were excluded from the data set before performing the analyses. Nevertheless, even larger sample sizes

may be required in future studies to obtain appropriate power and avoid parameter biases in SEM (see Supplementary Fig. S1). Note however that simple models, as used here, require smaller samples (e.g., about 30 cases for a simple CFA with four indicator variables) and larger samples are often only necessary if missing values exist³⁵. The robustness of the findings was further tested by conducting an additional analysis with an alternative parcellation scheme. Even though we were able to replicate the increased local efficiency and clustering in core regions of the implicit emotion regulation network, effects in the insula were weaker and those in ventromedial prefrontal cortex and frontal pole more pronounced. The present study focused on static functional connectivity, not considering the dynamic changes that functional connectivity may show across time, e.g., across the duration of MRI data acquisition. Increasingly, it is suggested that dynamics of functional connectivity are related to behavior and psychopathology³⁶, making it a worthwhile target for potential future studies investigating emotion dysregulation in ADHD.

In conclusion, the present study shows a positive relation of the right insula's clustering and local efficiency with emotion dysregulation in young adult individuals with ADHD-C/H. A similarly strong connection was not found for individuals with ADHD-I or healthy controls. The results suggest ADHD-type specific deficiencies in network forming processes that are associated with emotion processing and its implicit regulation. The commonly observed emotional problems in ADHD may partially be linked to the present findings. Given that emotion dysregulation is present in many other psychiatric disorders it is interesting to note that several of those, i.e. major depressive disorder, bipolar disorder, anxiety disorders and schizophrenia are also associated with changes in the structural and functional connectivity of the insula³⁷, which may represent a worthwhile target area for future treatment efforts.

Methods and materials

Participants and procedures. Data were taken from NeuroIMAGE II, the third wave of an integrated genetics-cognition-MRI-phenotype project on ADHD³⁸. It includes resting-state fMRI data of 249 individuals with ADHD as well as age- and sex-matched healthy controls. Initial recruitment criteria for ADHD participants were an ADHD combined type diagnosis, availability of one or more siblings, age between 6 and 18 years and availability of subject, sibling, and at least one biological parent for DNA collection. Exclusion criteria (for all participants) were IQ (as measured by Wechsler Intelligence Scale for Children/Wechsler Adult Intelligence Scale) < 70, diagnoses of autism or schizophrenia, and neurological disorders. For controls, it was required that neither they nor any of their first-degree relatives had a prior ADHD diagnosis.

Reassessment of the ADHD diagnosis was established by combining information from the Kiddie Schedule for Affective Disorders (K-SADS)³⁹ and parent, teacher, and self-report versions of the Conners' rating scale (CPRS-R:L, CTRS-R:L and CAARS-R:L)^{40–42}. Both the K-SADS and the Conners' rating scales provide operational definitions of the 18 behavioral ADHD symptoms defined in the DSM-IV. In both, symptoms are subdivided by symptom type, i.e., inattentive symptoms and hyperactive-impulsive symptoms. All diagnostic and phenotypic data was acquired on the same day as the fMRI data. A detailed description of the diagnostic procedures is given by von Rhein et al.³⁸.

Participants with a subthreshold ADHD diagnosis (2–4 ADHD-specific symptoms), left-handedness, excessive movement during the scanning, or insufficient quality of rs-fMRI or questionnaire data were excluded. 147 participants were used for the final analysis, including 31 participants with ADHD but without hyperactivity-impulsivity symptoms, i.e., predominantly inattentive ADHD (ADHD-I), 25 participants with ADHD and hyperactivity-impulsivity symptoms (ADHD-C/H), i.e., 21 with combined type ADHD and 4 with predominantly hyperactive-impulsive ADHD, and 91 healthy controls. Demographic information are given in Table 1.

Forty-eight hours prior to testing, stimulant medication use was discontinued. Data acquisition took place at the Donders Institute for Cognitive Neuroimaging, Radboud University Nijmegen, Netherlands. Participants (and their parents when < 18 years old) gave written informed consent for participation. In accordance with relevant guidelines and regulations, ethical approval was granted by the regional ethics board (Centrale Commissie Mensgebonden Onderzoek: CMO Regio Arnhem Nijmegen, ABR: NL41950.091.12). Data analysis was pre-registered using the open science framework (osf.io/rdyp6)⁴³.

Resting-state fMRI data acquisition and preprocessing. Whole-brain imaging was performed on a 1.5 T Magnetom Avanto (Siemens AG, Erlangen, Germany). BOLD-sensitive resting-state functional volumes were acquired using a T2*-weighted EPI sequence (TR = 1960 ms, TE = 40 ms). Each of the 266 volumes consisted of 37 axial slices of size 64 × 64 (flip angle = 80°, FoV = 224 × 224 mm², voxel-size = 3.5 × 3.5 × 3.0 mm³, interslice gap = 0.5 mm). T1-weighted high-resolution structural volumes were acquired with an MPRAGE sequence (TR = 2730 ms, TE = 2.95 ms, TI = 900 ms, flip angle = 9°, FoV = 256 × 256 mm², voxel-size = 1.0 × 1.0 × 1.0 mm³, GRAPPA 2).

Preprocessing mostly relied on FMRIB algorithms (FSL 5.0.11, <https://fsl.fmrib.ox.ac.uk/fsl/>)⁴⁴. The resting-state time series data were skull stripped, realigned to the middle volume of the series, co-registered to the structural T1, and spatially smoothed using a 6 mm full width at half maximum Gaussian kernel (FWHM). ICA-AROMA⁴⁵ was used to account for secondary movement artefacts. Residual noise was further reduced by nuisance regression including a linear trend and average times series measured within the white matter and cerebrospinal fluid. High-pass filtering was conducted at 0.008 Hz. Prior to network analysis, time series were warped to MNI152 space (Montreal Neurological Institute, Montreal, Canada). Root mean squared framewise displacement was calculated. A threshold of 0.25 was applied to exclude 25 participants with extreme movement from further analysis. Root mean squared framewise displacement did not significantly differ between the groups (healthy controls: 0.087 ± 0.071; ADHD-I: 0.128 ± 0.096; ADHD-C/H: 0.111 ± 0.096).

Graph analysis. For graph analysis we used Python 3.5 (version 3.5.10, <https://www.python.org>) with NetworkX (version 2.2, <https://networkx.org>)⁴⁶. Parcellation of preprocessed time series data was realized using a hemisphere-specific functional brain template with 268 parcels⁴⁷. It was created using graph-theory based parcellation that ensures functional homogeneity within the parcels of the atlas, even across different individuals. The atlas thus minimizes the likelihood that different functional areas lie within a single parcel⁴⁷. For 221 relevant parcels, covered by the MR measurement, subject-specific average intensity time series were calculated. Correlation matrices were created by computing pairwise Pearson's correlations between the extracted time series. Matrices were Fisher's z-transformed and absolute values were taken. Absolute value transformation was performed as preprocessing of the present data did not involve global signal regression and as anti-correlations are thought to be functionally relevant⁴⁸. Due to the naturally low density of negative correlations, we refrained from performing specific analysis for positive and negative correlations. To distinguish differences in network density from those of network topology⁴⁹, matrices were binarized based on seven equally spaced density thresholds with a minimum density of 0.10 and maximum density of 0.40⁵⁰. In this range of low to medium network densities, previous studies found significant associations between network topology and ADHD symptoms^{10,11,13}. Thus, seven threshold-specific graphs for each subject were investigated in the following graph analysis. Nodal topology measures were calculated for 70 of the 221 nodes. These 70 nodes were chosen based on their association with parcels overlapping with the orbitofrontal cortex, dorsolateral prefrontal cortex, ventromedial prefrontal cortex, anterior cingulate cortex, posterior parietal cortex, insula, ventral striatum, amygdala, and hippocampus as defined by the Harvard–Oxford Brain Atlas by more than 30%. These brain regions have been previously documented to be involved in emotion processing, its regulation, and brain dysfunctions in ADHD⁶.

Here, we captured the centrality of each node and analyzed whether nodes were highly integrated and connected, either locally towards their direct neighboring nodes or globally with the entire network. Thus, our focus is on six nodal measures, that is betweenness, closeness, eigenvector centrality, clustering coefficient, nodal efficiency, and local efficiency, which were used in previous studies on ADHD and showed ADHD-specific deviations^{10,11,13}. Betweenness, closeness, and eigenvector centrality are measures that describe the centrality of a node within a network. While betweenness describes how often a node is part of the shortest path between two other nodes, closeness describes how many of the theoretically possible direct connections to other nodes actually exist. Eigenvector centrality also considers the centrality of the node's direct neighbors. The clustering coefficient of a node describes how strongly its neighboring nodes are interconnected. Efficiency values indicate how directly nodes can be reached from other nodes of the network. In the case of nodal efficiency, this refers to the shortest connection from a particular node to all other nodes, while in the case of local efficiency it refers to the efficiency amongst the nodes adjacent to a particular node of interest. See Supplementary Fig. S2 for a more detailed description of the topology measures. All measures entered into separate SEM models described in 2.4.

Density-integrated topology measures were calculated⁴⁹. Differences between populations of weighted networks may be due to the networks' wiring costs and not the targeted topological features. Density-integration of measures from binarized networks, however, can eliminate cost-related differences and also allow the assessment of topology measures under different density-thresholds. Figure 2 summarizes the functional connectivity and network analysis.

Statistical analysis and structural equation modeling. *Variable selection.* Statistical analyses were conducted with R software (version 3.6.0, <https://cran.r-project.org/>)⁵¹. Lavaan (version 0.6-8, <https://lavaan.ugent.be/>) was used for SEM⁵². Prior to SEM, multi-group confirmatory factor analysis was used to identify data suitable for calculation of the latent emotion dysregulation variable. NeuroIMAGE II includes 6 tasks, questionnaires, or questionnaire subscales, respectively, that gauge emotional problems, emotional lability, and associated features: the Kessler Psychological distress scale, NESDA version of K-10⁵³ with 10 items for the assessment of emotional problems including anxiety and depression, the strength and difficulties questionnaire subscales (SDQ; five items about anxieties, worries, happiness, and physical symptoms of emotional stress for the emotional symptoms subscale and five items about temper tantrums, compliance, quarrelsomeness, stealing, and lying for the conduct symptoms subscales)⁵⁴, the emotional lability subscale of the Conners' parent rating scale (CPRS-R:L consisting of three items for unpredictable mood changes, temper tantrums, and tearfulness)⁴², the Inventory of Callous-Unemotional traits (ICU)⁵⁵ (24 items with a callousness and unemotional traits score), and the MINDS Testmanager's gradual emotion recognition task (GERT)⁵⁶ (accuracy of correct emotion classification).

Mediation structural equation model. The latent variable was used to investigate the relationship between functional brain network activity, emotion dysregulation, and ADHD. In the initial, preregistered analysis plan, we intended to use SEM mediation models in which the relationship between topological measures and the emotional latent variable was mediated by ADHD scores (CPRS-R:L) without taking into account the different ADHD presentations. However, those models did not produce good model-fit (as measured by the standard goodness-of-fit measures described below) and had no significant results. One reason may be that the ADHD scores were derived from a parents' questionnaire for children's ADHD symptoms (CPRS-R:L) which may be less valid than a clinical diagnosis.

Three-group structural equation model. Alternatively, we chose a multi-group SEM approach using the clinical diagnoses. The diagnoses reflect all available diagnostic information and may thus provide more accurate models. We investigated the group dependent differences (i.e., healthy controls, ADHD-I participants, and ADHD-C/H participants) in the association between topology measures and the latent variable gauging emotion dysregulation. Note, that by investigating group-related differences we aimed to identify associations between

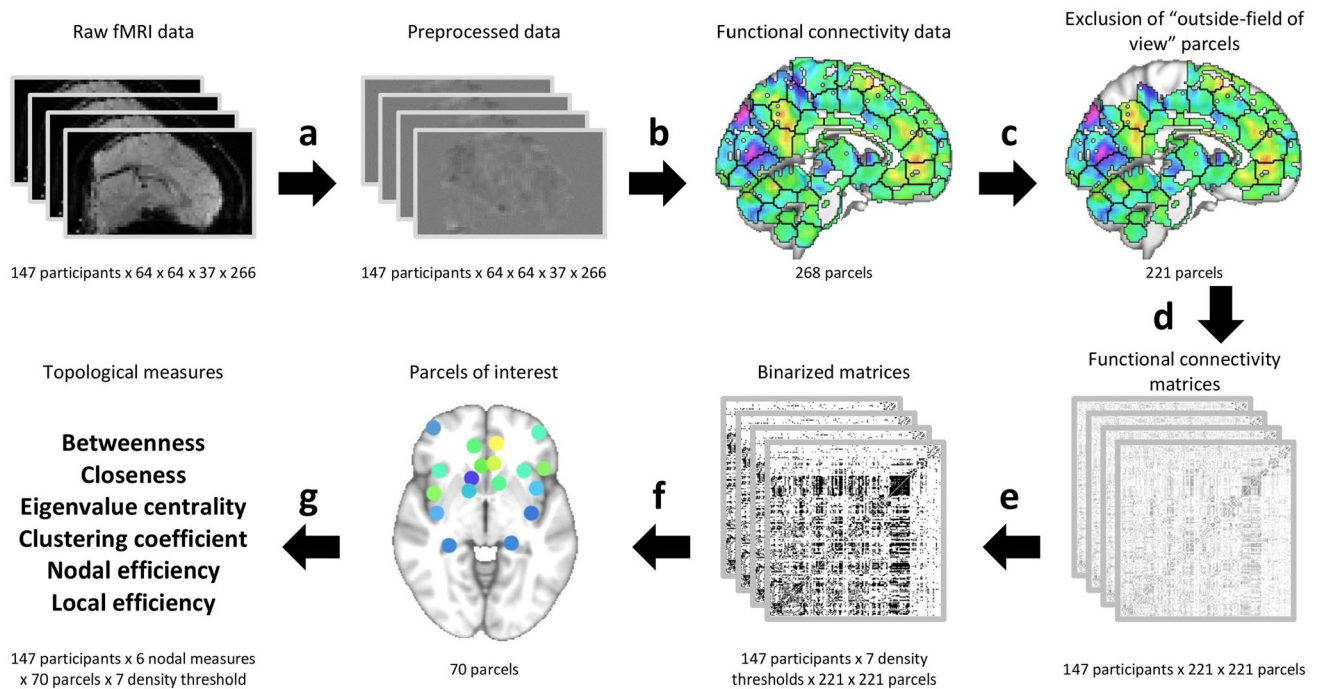


Figure 2. Resting-state functional connectivity analysis pipeline. Preprocessing included skull stripping, co-registration to structural images, realignment to middle volume, spatial smoothing (6 mm FWHM), ICA-AROMA, high-pass filtering (0.008 Hz), nuisance regression, and MNI152-space warping (a). Mean activation time series for parcels of functional connectivity template^{20,21} were extracted after exclusion of “outside-of-view” parcels (90% of the time 80% of voxels in a parcel had to have an intensity of > 1000) (b, c). Individual Fisher’s z-transformed correlation matrices were created (d). Each correlation matrix was binarized using 7 different density thresholds (0.10, 0.15, 0.20, 0.25, 0.30, 0.35, 0.40) (e). Graphs were created based on binarized matrices and for 70 relevant nodes. Density-integrated as well as threshold-specific topological network measures were calculated (f, g). Figure was created using FSLeaves (version 0.22.6, <https://fsl.fmrib.ox.ac.uk/fsl/fslwiki/FSLeaves>) and R software (version 3.6.0, <https://cran.r-project.org/>).

inter-individual differences in local brain network topology and emotional dysregulation that are specific for individuals with different ADHD presentation. This is different from a mediation model approach (see above) that aims to identify brain regions whose significant correlation with emotional dysregulation only reflects an indirect link via ADHD severity and thus might not directly involve emotion regulation. For each node of interest and each density-specific topology measure, one multi-group model was built. Models consisted of the latent variable, questionnaire scores, associated parameter estimates and variances as well as the nodal topology measure variable with its regression parameter for the latent variable (see Fig. 3). Factor loadings of the latent variable were fixed across groups, latent variable variance was standardized, and to account for between-group mean differences, group-specific intercepts were added. Models were compared with almost identical models, in which however the regression parameters between the network topology variable and the latent emotion dysregulation variable were fixed across groups. Model estimation was conducted using maximum likelihood procedures. To evaluate the significance of the group effects, model-specific χ^2 -values were compared between the two models (χ^2 -difference-test). Following the approach of Ginestet et al.⁴⁹, a model was considered significant if it revealed a significant effect on the density-integrated level (averaged over densities). Subsequently, significance was tested on each density threshold to provide detailed information on whether effects were found with stronger or weaker network connections.

Post-hoc analysis, multiple comparison procedures and goodness-of-fit. We used post-hoc two-group SEMs with Bonferroni-corrected *p*-values to investigate pairwise between-group differences. These two-group models resembled the three-group models described above, except that each only considered participants from two of the three groups. Alpha inflation due to multiple comparisons was controlled by the Benjamini–Hochberg false discovery rate (FDR) procedure⁵⁷. The comparative fit index (CFI), standardized root mean square residual (SRMR), and root mean square error of approximation (RMSEA) were calculated to evaluate the models’ goodness-of-fit. Acceptable goodness-of-fit measures should at least be above 0.95 for the CFI, below 0.08 for the SRMR, and below 0.10 for the RMSEA⁵⁸.

Additional analyses. To further control the robustness of the results, we evaluated whether group-specific differences in overall connectivity strength of the underlying adjacency matrices exist⁵⁹. Furthermore, an alternative parcellation scheme was used to investigate the robustness of the results with respect to the chosen parcel-

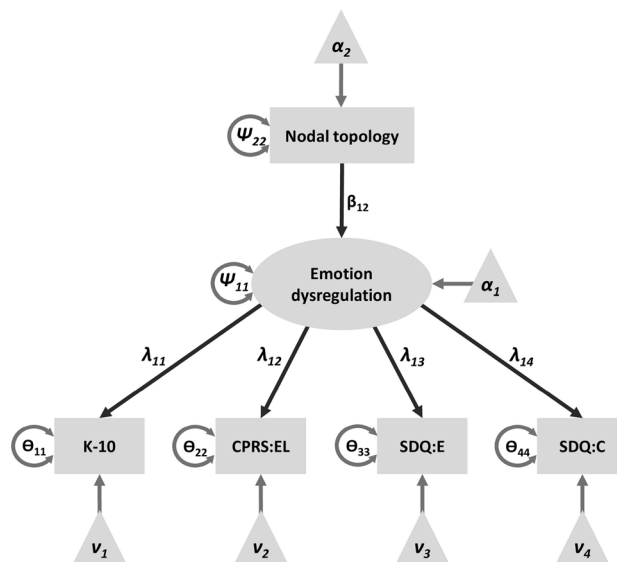


Figure 3. Multi-group structural equation model. Variances (V_1 – V_6) and intercepts (I_1 – I_6) are group specific. Loading parameters (p_1 – p_4) are fixed across groups while the regression parameter (p_5) is group specific. The model is compared to a model with fixed p_5 ; LV: latent variable for emotion dysregulation; K-10: Kessler Psychological distress scale, NESDA version of K-10; CPRS: EL: Conners' parent rating scale, revised, long version, emotional lability subscale; SDQ: E: Strength and Difficulties Questionnaire, emotional symptoms subscale; SDQ: C: Strength and Difficulties Questionnaire, conduct symptoms subscale. Figure was created using Microsoft PowerPoint 2016 MSO (version 16.0.4266.1001, <https://www.microsoft.com/de-de/microsoft-365/powerpoint>).

lation approach. For this, we used the AAL atlas⁶⁰, further subdivided with K-mean clustering to adapt the size and number of parcels to that of Finn et al.⁴⁷. Procedures for calculating topology measures and SEM analyses were conducted as described above.

Data availability

The data are property of the Donders Institute for Cognitive Neuroimaging and are available on request from the corresponding author. The data are not publicly available due to privacy or ethical restrictions. Further information about the NeuroIMAGE Project may be requested via the Project leader Jan K. Buitelaar.

Received: 2 February 2021; Accepted: 7 July 2021

Published online: 22 July 2021

References

1. Faraone, S. V. *et al.* Attention-deficit/hyperactivity disorder. *Nat. Rev. Dis. Prim.* **1**, 15020 (2015).
2. Shaw, P., Stringaris, A., Nigg, J. & Leibenluft, E. Emotion dysregulation in attention deficit hyperactivity disorder. *Am. J. Psychiatry* <https://doi.org/10.1176/appi.ajp.2013.13070966> (2014).
3. Carpenter, R. W. & Trull, T. J. Components of emotion dysregulation in borderline personality disorder: A review. *Curr. Psychiatry Rep.* <https://doi.org/10.1007/s11920-012-0335-2> (2013).
4. Maedgen, J. W. & Carlson, C. L. Social functioning and emotional regulation in the attention deficit hyperactivity disorder subtypes. *J. Clin. Child Psychol.* **29**, 30–42 (2000).
5. Etkin, A., Büchel, C. & Gross, J. J. The neural bases of emotion regulation. *Nat. Rev. Neurosci.* **16**, 693–700 (2015).
6. Rubia, K. Cognitive neuroscience of attention deficit hyperactivity disorder (ADHD) and its clinical translation. *Front. Hum. Neurosci.* **12**, 100 (2018).
7. Bos, D. J. *et al.* Structural and functional connectivity in children and adolescents with and without attention deficit/hyperactivity disorder. *J. Child Psychol. Psychiatry* **58**, 810–818 (2017).
8. Ho, N.-F. *et al.* Intrinsic affective network is impaired in children with attention-deficit/hyperactivity disorder. *PLoS ONE* **10**, e0139018 (2015).
9. Posner, J. *et al.* Dissociable attentional and affective circuits in medication-naïve children with attention-deficit/hyperactivity disorder. *Psychiatry Res. Neuroimaging* **213**, 24–30 (2013).
10. Lin, P. *et al.* Global and local brain network reorganization in attention-deficit/hyperactivity disorder. *Brain Imaging Behav.* **8**, 558–569 (2014).
11. Marcos-Vidal, L. *et al.* Local functional connectivity suggests functional immaturity in children with attention-deficit/hyperactivity disorder. *Hum. Brain Mapp.* **39**, 2442–2454 (2018).
12. Tomasi, D. & Volkow, N. D. Abnormal functional connectivity in children with attention-deficit/hyperactivity disorder. *Biol. Psychiatry* **71**, 443–450 (2012).
13. Wang, L. *et al.* Altered small-world brain functional networks in children with attention-deficit/hyperactivity disorder. *Hum. Brain Mapp.* **30**, 638–649 (2009).
14. Herpertz, S. C. *et al.* Emotional processing in male adolescents with childhood-onset conduct disorder. *J. Child Psychol. Psychiatry* **49**, 781–791 (2008).

15. Brotman, M. A. *et al.* Amygdala activation during emotion processing of neutral faces in children with severe mood dysregulation versus ADHD or bipolar disorder. *Am. J. Psychiatry* **167**, 61–69 (2010).
16. Posner, J. *et al.* The attenuation of dysfunctional emotional processing with stimulant medication: An fMRI study of adolescents with ADHD. *Psychiatry Res.* **193**, 151–160 (2011).
17. Spencer, A. E. *et al.* Abnormal fear circuitry in attention deficit hyperactivity disorder: A controlled magnetic resonance imaging study. *Psychiatry Res. Neuroimaging* **262**, 55–62 (2017).
18. Materna, L. *et al.* Adult patients with ADHD differ from healthy controls in implicit, but not explicit, emotion regulation. *J. Psychiatry Neurosci.* **44**, 340–349 (2019).
19. Sonuga-Barke, E. J. S. The dual pathway model of AD/HD: An elaboration of neuro-developmental characteristics. *Neurosci. Biobehav. Rev.* **27**, 593–604 (2003).
20. Hulvershorn, L. A. *et al.* Abnormal amygdala functional connectivity associated with emotional lability in children with attention-deficit/hyperactivity disorder. *J. Am. Acad. Child Adolesc. Psychiatry* **53**, 351–361.e1 (2014).
21. Yu, X. *et al.* Integrity of amygdala subregion-based functional networks and emotional lability in drug-naïve boys With ADHD. *J. Atten. Disord.* <https://doi.org/10.1177/1087054716661419> (2016).
22. Gogolla, N. The insular cortex. *Curr. Biol.* **27**, R580–R586 (2017).
23. Clark, L. *et al.* Differential effects of insular and ventromedial prefrontal cortex lesions on risky decision-making. *Brain* **131**, 1311–1322 (2008).
24. Fair, D. A. *et al.* Functional brain networks develop from a “local to distributed” organization. *PLoS Comput. Biol.* **5**, e1000381 (2009).
25. Giessing, C., Thiel, C. M., Alexander-Bloch, A. F., Patel, A. X. & Bullmore, E. T. Human brain functional network changes associated with enhanced and impaired attentional task performance. *J. Neurosci.* **33**, 5903–5914 (2013).
26. Castellanos, F. X. & Aoki, Y. Intrinsic functional connectivity in attention-deficit/hyperactivity disorder: A science in development. *Biol. Psychiatry Cogn. Neurosci. Neuroimaging* **1**, 253–261 (2016).
27. Sripada, C. S., Kessler, D. & Angstadt, M. Lag in maturation of the brain’s intrinsic functional architecture in attention-deficit/hyperactivity disorder. *Proc. Natl. Acad. Sci. U. S. A.* **111**, 14259–14264 (2014).
28. Qian, X. *et al.* Large-scale brain functional network topology disruptions underlie symptom heterogeneity in children with attention-deficit/hyperactivity disorder. *NeuroImage Clin.* **21**, 149 (2019).
29. Fair, D. A. *et al.* Distinct neural signatures detected for ADHD subtypes after controlling for micro-movements in resting state functional connectivity MRI data. *Front. Syst. Neurosci.* **6**, 80 (2013).
30. Blaskey, L. G., Harris, L. J. & Nigg, J. T. Are sensation seeking and emotion processing related to or distinct from cognitive control in children with ADHD?. *Child Neuropsychol.* **14**, 353–371 (2008).
31. Lindell, A. K. Continuities in emotion lateralization in human and non-human primates. *Front. Hum. Neurosci.* **7**, 464 (2013).
32. Koglin, U. & Petermann, F. Callous-unemotional traits: Verhaltensprobleme und prosoziales Verhalten bei Kindergartenkindern. *Kindheit und Entwicklung* **21**, 141–150 (2012).
33. Legenbauer, T. *et al.* Proper emotion recognition, dysfunctional emotion regulation. *Z. Kinder. Jugendpsychiatr. Psychother.* **46**, 7–16 (2018).
34. Sjöwall, D., Roth, L., Lindqvist, S. & Thorell, L. B. Multiple deficits in ADHD: Executive dysfunction, delay aversion, reaction time variability, and emotional deficits. *J. Child Psychol. Psychiatry* **54**, 619–627 (2013).
35. Wolf, E. J., Harrington, K. M., Clark, S. L. & Miller, M. W. Sample size requirements for structural equation models: An evaluation of power, bias, and solution propriety. *Educ. Psychol. Meas.* **76**, 913 (2013).
36. Rabany, L. *et al.* Dynamic functional connectivity in schizophrenia and autism spectrum disorder: Convergence, divergence and classification. *NeuroImage Clin.* **24**, 101966 (2019).
37. Namkung, H., Kim, S.-H. & Sawa, A. The insula: An underestimated brain area in clinical neuroscience, psychiatry, and neurology. *Trends Neurosci.* **40**, 200–207 (2017).
38. von Rhein, D. *et al.* The NeuroIMAGE study: A prospective phenotypic, cognitive, genetic and MRI study in children with attention-deficit/hyperactivity disorder. Design and descriptives. *Eur. Child Adolesc. Psychiatry* **24**, 265–281 (2015).
39. Kaufman, J. *et al.* Schedule for affective disorders and schizophrenia for school-age children-present and lifetime version (K-SADS-PL): Initial reliability and validity data. *J. Am. Acad. Child Adolesc. Psychiatry* **36**, 980–988 (1997).
40. Conners, C. K. *et al.* Self-ratings of ADHD symptoms in adults I: Factor structure and normative data. *J. Atten. Disord.* **3**, 141–151 (1999).
41. Conners, C. K., Sitarenios, G., Parker, J. D. & Epstein, J. N. Revision and restandardization of the Conners teacher rating scale (CTRS-R): Factor structure, reliability, and criterion validity. *J. Abnorm. Child Psychol.* **26**, 279–291 (1998).
42. Conners, C. K., Sitarenios, G., Parker, J. D. A. & Epstein, J. N. The revised Conners’ parent rating scale (CPRS-R): Factor structure, reliability, and criterion validity. *J. Abnorm. Child Psychol.* **26**, 257–268 (1998).
43. Foster, E. D. & Deardorff, A. Open science framework (OSF). *J. Med. Libr. Assoc.* **105**, 203 (2017).
44. Jenkinson, M., Beckmann, C. F., Behrens, T. E. J., Woolrich, M. W. & Smith, S. M. FSL—Review. *Neuroimage* <https://doi.org/10.1016/j.neuroimage.2011.09.015> (2012).
45. Pruim, R. H. R. *et al.* ICA-AROMA: A robust ICA-based strategy for removing motion artifacts from fMRI data. *Neuroimage* **112**, 267–277 (2015).
46. Hagberg, A., Schult, D. A. & Swart, P. J. *Exploring Network Structure, Dynamics, and Function using NetworkX* (2008).
47. Finn, E. S. *et al.* Functional connectome fingerprinting: Identifying individuals using patterns of brain connectivity. *Nat. Neurosci.* **18**, 1664–1671 (2015).
48. Murphy, K., Birn, R. M., Handwerker, D. A., Jones, T. B. & Bandettini, P. A. The impact of global signal regression on resting state correlations: Are anti-correlated networks introduced?. *Neuroimage* **44**, 893–905 (2009).
49. Ginestet, C. E., Nichols, T. E., Bullmore, E. T. & Simmons, A. Brain network analysis: Separating cost from topology using cost-integration. *PLoS ONE* **6**, e21570 (2011).
50. Achard, S. & Bullmore, E. Efficiency and cost of economical brain functional networks. *PLoS Comput. Biol.* **3**, e17 (2007).
51. R Core Development Team. *R: A Language and Environment for Statistical Computing* (R Found. Stat. Comput., 2016). <https://doi.org/10.1007/978-3-540-74686-7>
52. Rosseel, Y. lavaan: An R package for structural equation modeling. *J. Stat. Softw.* **48**, 1–36 (2012).
53. Penninx, B. W. J. H. *et al.* The Netherlands study of depression and anxiety (NESDA): Rationale, objectives and methods. *Int. J. Methods Psychiatr. Res.* **17**, 121–140 (2008).
54. van Widenfelt, B. M., Goedhart, A. W., Treffers, P. D. A. & Goodman, R. Dutch version of the strengths and difficulties questionnaire (SDQ). *Eur. Child Adolesc. Psychiatry* **12**, 281–289 (2003).
55. Kimonis, E. R. *et al.* Assessing callous-unemotional traits in adolescent offenders: Validation of the Inventory of callous-unemotional traits. *Int. J. Law Psychiatry* **31**, 241–252 (2008).
56. Brand, N., Von Borries, K. & Bulten, E. Progress with MINDS, a testmanager for psychological assessment, research and education: Applications in the forensic psychiatric domain. In *Proceedings of Measuring Behavior 2010 (Eindhoven, The Netherlands)* (eds Spink, A. J., Grieco, F., Krips, O. E., Loyens, L. W. S., Noldus, P. J. J. & Zimmerman, P. H.) 396–398 (2010) (accessed 15 October 2019); <https://www.mindsware.nl/introductie/>.

57. Benjamini, Y. & Hochberg, Y. Controlling the false discovery rate: A practical and powerful approach to multiple testing. *J. R. Stat. Soc. Ser. B* **57**, 289–300 (1995).
58. Schermelleh-Engel, K., Moosbrugger, H. & Müller, H. H. Evaluating the fit of structural equation models: Tests of significance and descriptive goodness-of-fit measures. *Methods Psychol. Res.* **8**, 23–74 (2003).
59. van den Heuvel, M. *et al.* Proportional thresholding in resting-state fMRI functional connectivity networks and consequences for patient-control connectome studies: Issues and recommendations. *Neuroimage* **152**, 437–449 (2017).
60. Tzourio-Mazoyer, N. *et al.* Automated anatomical labeling of activations in SPM using a macroscopic anatomical parcellation of the MNI MRI single-subject brain. *Neuroimage* **15**, 273–289 (2002).

Acknowledgements

The NeuroIMAGE Project was supported by NWO Large Investment Grant 175.010.2007.0100, ZonMw Addiction: Risk Behaviour and Dependency Grant 31160209, NWO MaGW Grant 433-09-242, NWO National Initiative Brain & Cognition Grant 056-13-015 (all to Jan K. Buitelaar), and ZonMw Priority Medicines Kinderen 113202005 Grant (to Pieter Hoekstra). Additional funding comes from the Radboud University Nijmegen Medical Center, University Medical Center Groningen and Accare, and VU University Amsterdam. Furthermore, funding was contributed by the European Union's Seventh Framework and Horizon 2020 Programmes under Grant agreement no 603016 (MATRICS) and 728018 (Eat2beNICE). This work reflects only the authors' views and the European Union is not liable for any use that may be made of the information contained herein. Tammo Viering is funded by the Oldenburg-Groningen Joint Graduate Research Training Group "Translational Research: From Pathological Mechanisms to Therapy". Jilly Naaijen is funded by a VENI Grant from the Dutch Organisation for Scientific Research (NWO).

Author contributions

T.V., P.J.H., A.P., C.G., and C.M.T. were involved in the general conceptualization of the Project. P.J.H., J.N., C.A.H., J.K.B. contributed to the data collection process. Methodology and study design were developed by T.V., P.J.H., A.H., C.G., and C.M. Thiel. The implementation of the analysis software as well as the execution of the analysis was done by T.V. T.V. wrote the initial draft of the manuscript and created all visualizations. All authors reviewed and edited the manuscript. Supervision was provided by P.J.H., J.N., C.G., and C.M.T. P.J.H., A.P., J.K.B., and C.M.T. contributed to the required resources. Financial support was acquired by P.J.H. and J.K.B. P.J.H., J.K.B., C.G., and C.M.T. contributed to the Project administration.

Funding

Open Access funding enabled and organized by Projekt DEAL.

Competing interests

Jan K. Buitelaar has been in the past 3 years a consultant to/member of advisory board of/and/or speaker for Shire, Roche, Medice, and Servier. He is not an employee of any of these companies, and not a stock shareholder of any of these companies. He has no other financial or material support, including expert testimony, patents, royalties. Dr Philipsen has been in the last year a member of advisory board and a speaker for Shire/Takeda, and Medice. She received travel support from Janssen-Cilag, Shire/Takeda. She is an author of books and articles on ADHD published by Elsevier, Hogrefe, Schattauer, Kohlhammer, Karger, and Oxford publishers. The other authors declare no further competing interests.

Additional information

Supplementary Information The online version contains supplementary material available at <https://doi.org/10.1038/s41598-021-94426-8>.

Correspondence and requests for materials should be addressed to T.V.

Reprints and permissions information is available at www.nature.com/reprints.

Publisher's note Springer Nature remains neutral with regard to jurisdictional claims in published maps and institutional affiliations.



Open Access This article is licensed under a Creative Commons Attribution 4.0 International License, which permits use, sharing, adaptation, distribution and reproduction in any medium or format, as long as you give appropriate credit to the original author(s) and the source, provide a link to the Creative Commons licence, and indicate if changes were made. The images or other third party material in this article are included in the article's Creative Commons licence, unless indicated otherwise in a credit line to the material. If material is not included in the article's Creative Commons licence and your intended use is not permitted by statutory regulation or exceeds the permitted use, you will need to obtain permission directly from the copyright holder. To view a copy of this licence, visit <http://creativecommons.org/licenses/by/4.0/>.

© The Author(s) 2021